

1 **Leaching of CEM III paste by demineralised or mineralised water at pH 7 in relation with aluminium**
2 **release in drinking water network**

3 Mathilde Berthomier^{1, 2, 3}, Christine Lors², Denis Damidot², Thomas De Larrard¹, Cyril Guérandel³,
4 Alexandra Bertron^{1,*}

5 1. LMDC, Université de Toulouse, UPS, INSA Toulouse, France

6 2. LGCgE, Université de Lille, IMT Lille Douai, France

7 3. SGR Paris, Saint-Gobain, Aubervilliers, France

8 *Corresponding author: INSA Toulouse, 135 avenue de Rangueil, 31077 Toulouse Cedex 4, France
9 bertron@insa-toulouse.fr

10 **Abstract**

11 Drinking water pipes can be lined with a cement matrix based on CEM III, which can release
12 aluminium into the water. However, the European Union limits the aluminium concentration in
13 drinking water for public health reasons. In order to study the long-term leaching mechanism of
14 aluminium, semi-dynamic leaching tests using an aggressive solution (demineralised water) or
15 drinking water (mineralised water) were conducted on crushed CEM III pastes maintained at pH 7.
16 They resulted in a very high leaching coefficient, approaching 50 %. However, in spite of this strong
17 leaching, the amount of Al leached remained very low, at less than 1.5 % of the initial amount of Al in
18 the material. Under these conditions, the leaching of Al from a CEM III paste is complex since it
19 involves several steps, where slag (1st and last steps) or cement paste (2nd step) are the main
20 contributors.

21 **Keywords:**

22 Leaching; cement paste; slag; drinking water

23 **1. Introduction**

24 A high consumption of aluminium can be dangerous for humans. For example, it can cause many
25 undesirable effects (encephalitis, bone diseases, anaemia) in dialysis patients, whose treatments are
26 very rich in aluminium [1]. It is also suspected of being related to Alzheimer's disease, even though
27 studies on the subject are currently contradictory and no causal link between aluminium
28 consumption and the onset of the disease has been demonstrated [2]–[7]. This is why the European
29 Union (EU, 98/83/CE) and the World Health Organization (WHO) recommend a concentration of less
30 than 200 µg/L in drinking water for this element. However, trace amounts of aluminium may be

31 naturally present in water and may come mainly from water treatment (aluminium salts used as
32 coagulant). Thus, the limit of 200 µg/L corresponds to the limit set for the optimization of the
33 coagulation process with aluminium-based coagulants used in drinking water treatment plants,
34 which is lower than the health-based guideline value of 900 µg/L [8].

35 Some pipelines used for the transport of drinking water consist of a cast iron pipe lined with blast
36 furnace cement mortar (CEM III), which is composed of Portland clinker and blast furnace [9]. The
37 flow of water in the pipe causes leaching of the lining, which leads to the release of chemical
38 elements contained in the mortar, including aluminium, into the drinking water. The presence of
39 blast-furnace slag in CEM III cement promotes the durability of the cementitious material by slowing
40 the leaching kinetics compared to a Portland cement mortar (CEM I), but the aluminium content of
41 the liner is increased [10] – [15]. Studies on the leaching of cementitious materials generally carried
42 out on CEM I-based materials have clearly highlighted the dissolution-precipitation mechanisms
43 involved in relation to kinetics governed by diffusion [16]–[23]. Thus, during the leaching of CEM I-
44 based materials, the departure of cementitious ions and a gradual dissolution of hydrates occurs. In
45 the material, the corresponding dissolution fronts progress in proportion to the square root of the
46 time in the case of a unidirectional geometry [24], [25]. Cementitious ion leaching studies focus
47 mainly on the release of the majority of CEM I ions, i.e. calcium and silicon ions. In addition, they are
48 generally based on fairly short tests leading to moderate leaching of the samples overall. During the
49 leaching of CEM III pastes [11], [13], [25]–[27], the dissolution-precipitation phenomena of the
50 cementitious phases are close to those observed during the leaching of CEM I pastes with, first of all,
51 a dissolution of the portlandite, followed by the sequential dissolution of the AFm and ettringite
52 together with the progressive decalcification of the C-S-H [24], [25], [28]. However, in CEM III-based
53 materials, much of the C-S-H contains aluminium and the leaching mechanisms of C-A-S-H are little
54 detailed in the literature or not at all. In addition, the leaching of aluminium, mainly present in AFm,
55 ettringite, C-A-S-H and residual anhydrous slag, has been little studied in the literature for CEM I and
56 CEM III matrices. The studies carried out by Bertron et al. on the leaching of cement pastes with
57 organic acids and by Müllauer et al. on the leaching of concrete with demineralised water showed a
58 higher relative release of aluminium during the leaching of a CEM III paste than during the leaching of
59 a CEM I paste in the short term [13], [29]. These results indicate that the mechanisms governing the
60 release of aluminium are more complex than those associated with the release of calcium, which are
61 governed by diffusion.

62 Thus, a specific investigation effort is required with respect to aluminium leaching in order to
63 estimate the impact of the presence of slag in cementitious materials in contact with drinking water.
64 In the light of the particular leaching behaviour of aluminium over time, tests to reach advanced

65 leaching stages should be carried out to determine the leaching behaviour of aluminium-rich solids.
66 So, to accelerate leaching without modifying the chemical reactions, leaching tests were run on
67 crushed materials. The interest of this type of test, performed on fine grains instead of a monolith, is
68 twofold: on the one hand, it makes it possible to limit the effect of diffusion on the leaching kinetics
69 and, on the other hand, it increases the surface area of the grains in contact with the solution, thus
70 increasing the release kinetics of the chemical elements in solution. However, the various studies on
71 the leaching of crushed cementitious materials were have been conducted under different conditions
72 from those corresponding to the release of chemicals into drinking water - either at an initial pH of 4
73 [29] or by varying the pH of the leach solution between 2 and 14 [30]–[32]. The purpose of the tests
74 carried out was to study the behaviour and stability of the material at different pH levels and the
75 solubilisation of chemical elements as a function of pH. The leaching tests were based on the
76 standard XP CEN/TS 14429 [33] for the studies by Engelsen et al., Lupsea et al., and Schiopu [30]–
77 [32].

78 The work reported in this article is intended to provide new data to investigate the mechanisms of
79 aluminium leaching from cementitious materials over the long term under conditions of pH close to
80 7. To achieve this, leaching tests were carried out at a pH maintained constant at 7, on crushed slag
81 cement pastes (CEM III/B) in the presence of demineralised water or mineralised water under semi-
82 dynamic conditions. Two leaching solutions were used in order to place one paste in aggressive
83 conditions with demineralised water and the other in more realistic conditions with a weakly
84 mineralised water having a composition that was average for a French drinking water. Additional
85 tests were conducted on anhydrous slag and Portland cement paste (CEM I) leaching using
86 demineralised water to estimate the contributions of the two materials in a simplified manner. The
87 amount of chemical elements leached according to the leaching time was calculated from ICP-OES
88 chemical analysis of the resulting leachate. The degraded materials were studied using scanning
89 electron microscopy coupled with energy dispersive spectroscopy (SEM-EDS), X-ray diffractometry
90 (XRD) and ²⁷Al nuclear magnetic resonance spectrometry (NMR) analyses to highlight their
91 microstructural, chemical and mineralogical evolution.

92

93 **2. Materials and methods**

94 **2.1. Cementitious materials**

95 Two commercial cements (from Ciments Calcia) were used in this study: one CEM I 52.5 , rated CEM
96 I, and one CEM III/B 32.5, rated CEM III, together with anhydrous blast furnace slag, rated slag

97 identical to that used to manufacture CEM III. Their chemical compositions are set out in Table 1.
 98 Cement CEM III was composed of 94% of binder (71% slag and 29 % clinker) and 6% setting regulator
 99 (according to the [technical data sheet provided by the cement manufacturer](#)), which corresponds to
 100 approximately 67% slag and 27% clinker in the total cement. The blast furnace slag was obtained
 101 following a rapid vitrification process which resulted in an essentially amorphous material. Thus, up
 102 to 98% of the studied slag was vitrified. The mineralogical analysis of this material revealed the
 103 presence of two phases crystallized in very small quantities: quartz and calcite. Specimens of CEM III
 104 and CEM I paste were made with a water/cement ratio of 0.31 for the CEM III paste and 0.4 for the
 105 CEM I paste, in order to have a sufficient quantity of water to carry out the mixing. The cementitious
 106 pastes were made using a standard mortar mixer according to the following mixing protocol: 30 s at
 107 low speed (140 rotations per minute), 30 s at high speed (285 rotations per minute), 90 s without
 108 rotation and then 60 s at high speed. After mixing, the moulds were half filled and vibrated for 1
 109 minute. They were then completed and vibrated again for 1 minute. The moulds were stored in a
 110 room at 20 °C. After 24 hours, the specimens were removed from the moulds and stored at 20 °C in a
 111 sealed plastic bag for a minimum of 27 days. The CEM III and CEM I pastes were kept for 16 months
 112 and 6 months in plastic bags, respectively, after their manufacture. They were then crushed just
 113 before the leaching experiments.

114 The cementitious pastes and slag used for the leaching tests were manually crushed with an agate
 115 mortar and then sieved at 500 µm to zero rejection. Figure 1 shows the particle size distribution and
 116 Table 2 shows the particle sizes (D10, D50 and D90) of the various crushed samples measured with a
 117 dry laser particle size analyser (Belckman Coulter LS 13 320). Manual grinding explains the
 118 differences between the grain sizes of the different samples. Thus, the slag, which is harder, had a
 119 coarser grain size than crushed cementitious pastes.

120 For the sampling of crushed cementitious pastes or anhydrous slag, quartering was performed in
 121 order to take 5 grams of powder with characteristics representative of the whole sample.

122 *Table 1: Chemical compositions of CEM I cement, CEM III cement and slag in percent by mass*

	CEM I	CEM III	Slag
CaO	64.31	49.13	42.38
SiO₂	20.12	29.60	37.74
Al₂O₃	5.56	9.41	11.09
Fe₂O₃	2.32	1.21	0.39
MgO	0.93	4.69	6.39

MnO	0.04	0.27	0.39
SO₃	3.82	3.22	0.09
P₂O₅	0.15	0.06	0.02
TiO₂	0.26	0.52	0.73
Na₂O	0.14	0.24	0.29
K₂O	0.95	0.59	0.44
Cl	0.04	0.02	0.01
Cr₂O₃	0.01	0.01	0.01
Ignition loss	1.38	1.02	0.00

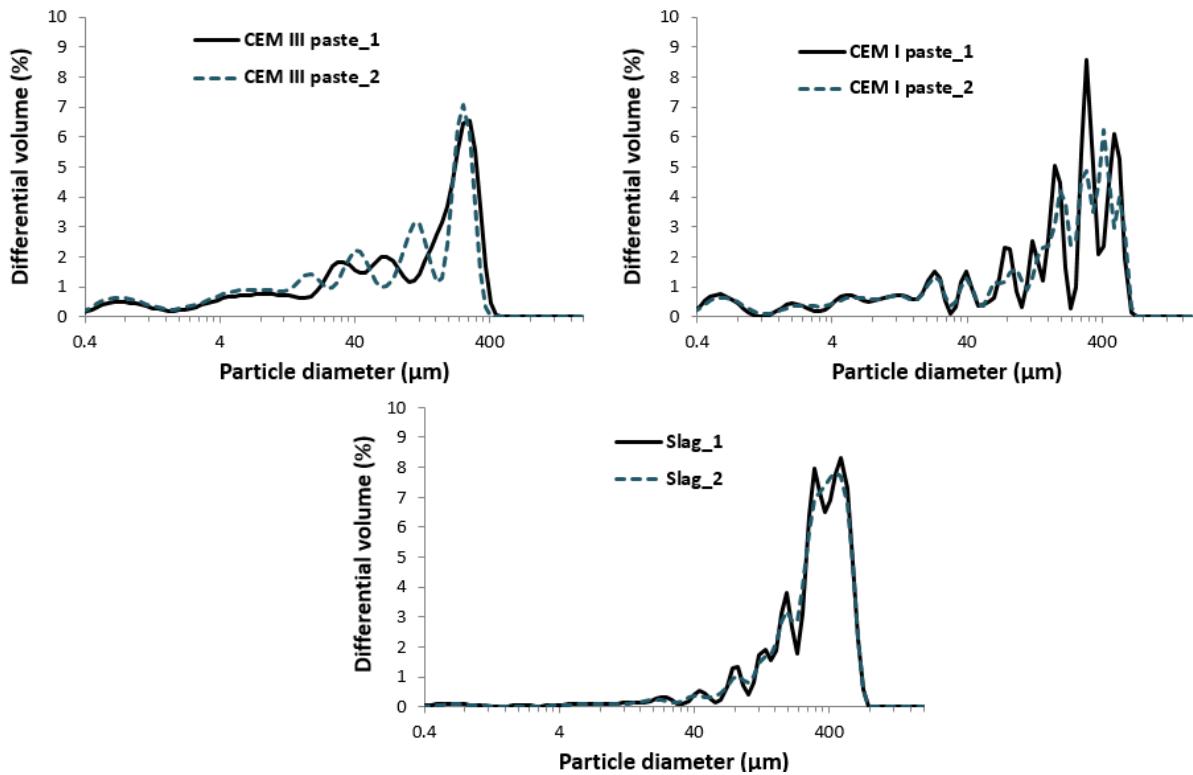
123

124

Table 2: Grain sizes (D10, D50 and D90) of crushed samples

	CEM III paste	Slag	CEM I paste
D₁₀ (μm)	4.3 ± 0.7	93.3 ± 3.6	5.1 ± 0.1
D₅₀ (μm)	105.2 ± 14.3	348.9 ± 0.9	194.5 ± 4.5
D₉₀ (μm)	303.7 ± 14.0	577.4 ± 1.1	507.9 ± 13.3

125



126

127

Figure 1: Particle size distribution of crushed samples

128

129

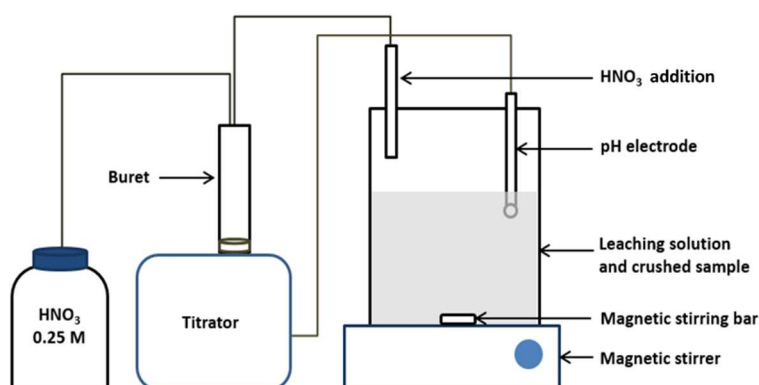
130 2.2. Methods

131 2.2.1. Leaching test

132 Semi-dynamic leaching tests were carried out on crushed cement paste and slag samples. Adapted
133 from Adenot [34], the principle of the test used was that of an accelerated leaching test
134 characterized by:

- 135 - maintaining the pH of the leaching solution by adding concentrated nitric acid at 0.250 mol/L
136 made by diluting nitric acid (HNO₃) at 2 mol/L (Fisher Scientific, France)
- 137 - regular renewal of the leaching solution (carried out as soon as a given quantity of acid had
138 been added to the solution or at a given time).

139 The experimental system consisted of a 2 L reactor containing 1 L of leaching solution and 5 g of
140 crushed sample. The reactor was equipped with a pH electrode and a buret connected to a titrator
141 (Radiometer Analytical TitraLab 854), in order to control and measure the pH of the solution
142 continuously (Figure 2). The reactor solution was kept under agitation by a magnetic stirrer. The pH
143 of the leach solution was maintained at 7 by adding nitric acid ([HNO₃] = 0.250 mol/L). The pH was
144 chosen in accordance with the European directive UE 98/83/CE that recommends the pH of a
145 drinking water should be comprised in the interval [6.5; 9.5]. The target pH was thus close to the
146 lower value of this interval. Moreover, it should be noted that the speciation of Al is the same on the
147 pH interval [5.5; 8]: Al(OH)₃ is the predominant specie [35] Moreover, the possible difference in
148 terms of chemical stability of the cementitious phases between our target pH 7 and the minimal pH
149 of potable water 6.5 should be considered as negligible [36]–[38].



150

151 *Figure 2: Diagram and photograph of the leaching test carried out on crushed samples*

152 Two types of leaching solutions were used:

- 153 - demineralised water (DW) (ELGA labWater purification system)
- 154 - weakly mineralised water (Volvic commercial water, pH 6.9). The composition of the
155 mineralised water was analysed by ICP-OES (Inductively Coupled Plasma - Optical Emission
156 Spectrometry, Varian 720-ES) for cation analysis and by ion chromatography (Dionex ICS-
157 3000 with an AG15 pre-column and an AS15 column with a flow rate of 1.2 ml KOH at 38
158 mM) for anion analysis (Table 3). The aluminium content of this water was below the
159 detection limit of 5 $\mu\text{mol/L}$.

160

161 The tests lasted 1 month and were carried out at a constant temperature of 30 °C. This temperature
162 was chosen to accelerate the diffusion kinetics and also the chemical reactions slightly without
163 changing the stability of the mineral phases present. The CEM III paste was leached with
164 demineralised water and mineralised water, and the slag and paste of CEM I were leached with
165 demineralised water.

166 *Table 3: Composition of mineralised water (mmol/L). DL: detection limit 5 $\mu\text{mol/L}$*

	Ca	Na	K	Mg	Si	Cl	SO ₃	HCO ₃	NO ₃	Al
Concentration (mmol/L)	0.317	0.559	0.179	0.351	0.546	0.421	0.105	1.278	0.113	<DL
Standard deviation	0.011	0.018	0.0057	0.012	0.019	0.003	0.001	0.010	0.003	/

167

168 A first renewal was performed after 2.5 hours, followed by a second renewal 16 hours after the first,
169 because of a very high release of chemical elements at the beginning of the test due to the large
170 specific surface of the sample. The following renewals were made every 3.5 days. For the CEM III
171 paste leached with DW, the renewals were spaced over the end of the experiment. Thus the total
172 number of renewals was 8, compared to 10 renewals for the other 3 experimental conditions.

173 A specific procedure was set up during the renewal of the leaching solution in order to limit the loss
174 of crushed solid sample during this step: the reactor, containing the leachate and the crushed solid,
175 was left to rest for a few minutes after the agitation was stopped, so that the crushed solid could
176 settle. Two hundred millilitres of leachate was then taken from the surface of the reactor and
177 distributed among 4 tubes of 50 mL. These tubes were centrifuged at 7500 RCF (6455 RPM) for 8
178 minutes (MF20/R Awel Centrifuge). The supernatant was removed and then centrifuged a second
179 time. The first half of the supernatant was collected and acidified to 0.2% HNO₃ at 67% concentration

180 and filtered through 0.45 μm . The second half was filtered at 0.45 μm and then acidified to 0.2%
181 HNO_3 at 67% concentration. These samples were then analysed by ICP-OES.

182 In parallel with the centrifugation, the rest of the mixture present in the reactor (mixture of leachate
183 and crushed cement paste) was filtered under vacuum at 0.45 μm in order to recover the solid part,
184 which was then redispersed in a new leaching solution.

185 **2.2.2. Leachate analyses**

186 The chemical composition of the leachate was determined by ICP-OES (Inductively Coupled Plasma -
187 Optical Emission Spectrometry, Varian 720-ES). The concentrations of the elements Ca, Si, Al, Mg
188 were analysed.

189 The elements were analysed using a nebuliser flow rate of 0.75 L/min and a generator power of 1200
190 W. In order to increase the analytical accuracy for aluminium in solution, the analytical method was
191 optimised. The optimisation made it possible to analyse, at least, aluminium concentrations (limits of
192 quantification) of 20 $\mu\text{g/L}$ when the analysed solution contained several elements. To achieve this, a
193 standard range of aluminium was produced with a matrix loaded with the following elements:
194 calcium (130 mg/L), silicon (6 mg/L), potassium (40 mg/L) and sodium (5 mg/L) at constant
195 concentrations.

196 **2.2.3. Analyses of cementitious materials**

197 Microstructural observations of the leached crushed materials by scanning electron microscope
198 (SEM, Jeol JSM-6380 LV and Hitachi S 4300 SE/N) were performed, coupled with chemical analysis by
199 EDS (Energy-Dispersive X-ray Spectroscopy, Bruker XFlash[®] 6/30 and Thermo Electron Ultradry Silicon
200 drift). For this purpose, the leached powder was dispersed in resin (resin and hardener Presi
201 Mecaprex Ma2+ or Araldite 2020), then polished (with silicon carbide discs having a grain size of 26
202 μm (600), 22 μm (800), 15 μm (1200), and 10 μm (2000), then with 9 μm , 6 μm and 1 μm diamond
203 paste), and metallized. During the chemical analysis of the material by EDS, about 30 points were
204 analysed in the cement paste and slag, in order to obtain an average composition.

205 X-ray diffraction mineralogical analyses (XRD, Bruker D8 advance with a copper anticathode, 40 kV
206 voltage and 40 mA current or Bruker D8 advance with a cobalt anticathode, 35 kV voltage and 40 mA
207 current) were performed on each of the initial crushed samples and the leached ones.

208 The analyses in MAS NMR spectroscopy of the ^{27}Al nucleus were performed at 208.48 MHz on a
209 Bruker AVANCE-III spectrometer (18.8 T) equipped with an HX-3.2 mm measuring probe. The
210 recordings were made at a rotational speed of 22 kHz with a pulse time of 0.5 μs and a

211 radiofrequency field of 30 kHz (measured on a liquid). 8192 accumulations were recorded with a
212 recycling time of 0.5 s. The spectra were corrected for the weak probe signal by subtracting the signal
213 recorded without a sample from the analyses performed.

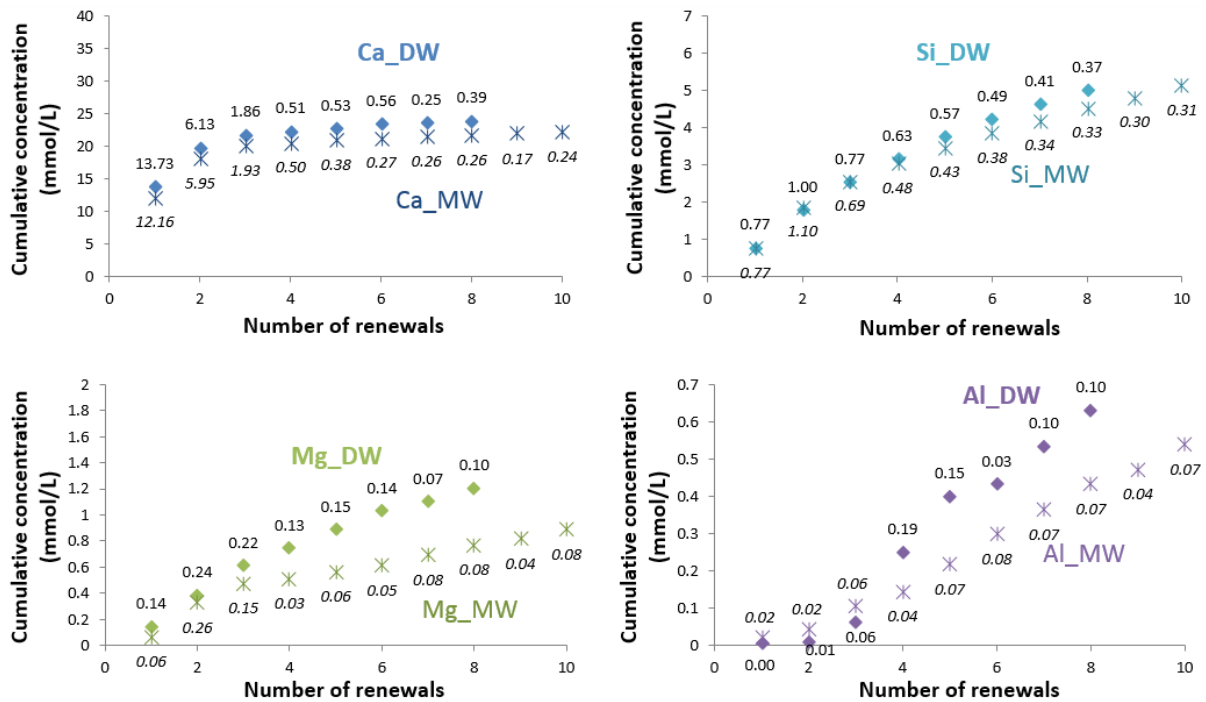
214

215 **3. Results**

216 **3.1. Leachate analysis**

217 Figure 3 shows the results obtained by leaching the crushed CEM III cement paste with demineralised
218 water (DW) and mineralised water (MW) for one month at 30 °C. Each point represents a renewal.
219 The figure shows very strong leaching of Ca at the beginning of the experiment, since 90 % of the
220 total leached calcium has been released by the 3rd renewal. Thereafter, a small additional amount of
221 calcium is released in solution. For Mg and Si, the total cumulative concentrations are twice the
222 concentration obtained at the 3rd renewal and the curves obtained have a polynomial appearance. A
223 different behaviour is observed for aluminium: only 10% of the total cumulative concentration is
224 leached by the 3rd renewal (5th day of the test). The quantity released is then almost linear
225 according to the number of renewals. A different behaviour is observed for aluminium: only 10% of
226 the total cumulative concentration is leached by the 3rd renewal (5th day of the test).

227 The test carried out with mineralised water shows results very close to those obtained for
228 demineralised water for Ca and Si, whose concentrations have similar trends. The final cumulative
229 concentrations for Ca are 23.9 mmol/L in the DW and 22.1 mol/L in the MW, and for Si, 4.9 mmol/L
230 in the DW and 5.1 mol/L in the MW. For Mg and Al, on the other hand, the differences between the
231 two solutions are a little more pronounced. On the one hand, the concentration evolution curves are
232 linear for the MW test, from the 3rd renewal for Mg and from the 1st renewal for Al. The difference
233 between the final concentrations is greater. For Mg, concentrations of 1.2 mmol/L for the DW test
234 and 0.8 mmol/L for the MW test were found, and for Al, concentrations were 0.63 mmol/L for the
235 DW test and 0.54 mmol/L for the MW test. Thus, Mg and Al are less leached in the MW.



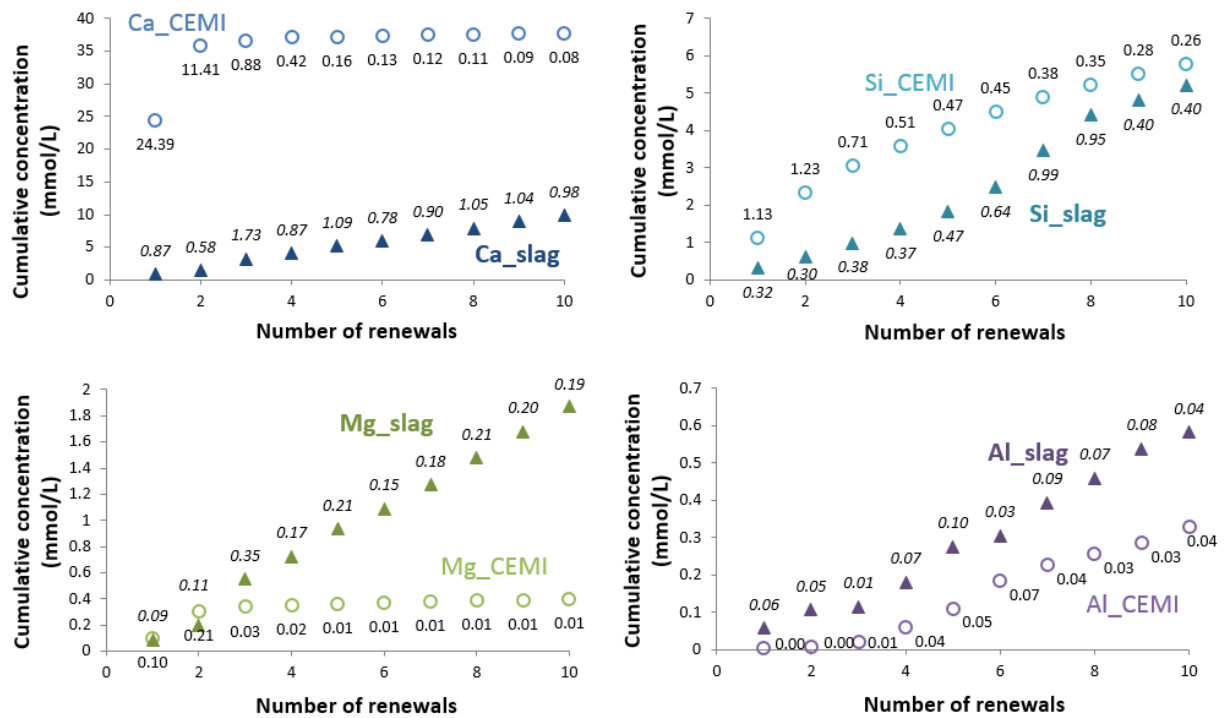
236

237 *Figure 3: Cumulative concentrations of leached elements during the leaching of the degraded crushed*
 238 *CEM III paste with demineralised water (DW) and mineralised water (MW) for one month at 30 °C*
 239 *according to the number of renewals. Each point represents a renewal of the leachate. The value*
 240 *associated with each point corresponds to the non-cumulative concentrations (mmol/L) analysed for*
 241 *each leachate*

242 Figure 4 shows the results obtained when leaching the crushed CEM I paste and the crushed slag
 243 with demineralised water for one month at 30 °C. The leaching of the CEM I paste shows results
 244 similar to those of the CEM III paste in terms of the Ca, Si and Al curves. However, the quantities of
 245 elements leached are significantly different. For CEM I paste leached with DW, the following
 246 concentrations were obtained at the end of the test: Ca = 37.8 mmol/L, Si = 5.8 mmol/L, Mg = 0.4
 247 mmol/L and Al = 0.33 mmol/L. The concentrations released are related to the quantities originally
 248 present in the material. Thus, unlike the quantities of Mg and Al, those of Ca and Si are higher for the
 249 leaching of CEM I paste than for the leaching of CEM III paste.

250 For slag, Ca and Mg leaching were almost linear during the number of renewals, with cumulative
 251 concentrations of 9.88 mmol/L for Ca and 1.87 mmol/L for Mg at the end of the test (Figure 4). In this
 252 test, Si and Al behaved similarly, with slow leaching of these elements during the first 10 days. The
 253 release of these elements then increased, to reach 5.21 mmol/L for Si and 0.58 mmol/L for Al at the
 254 end of the test.

255



256

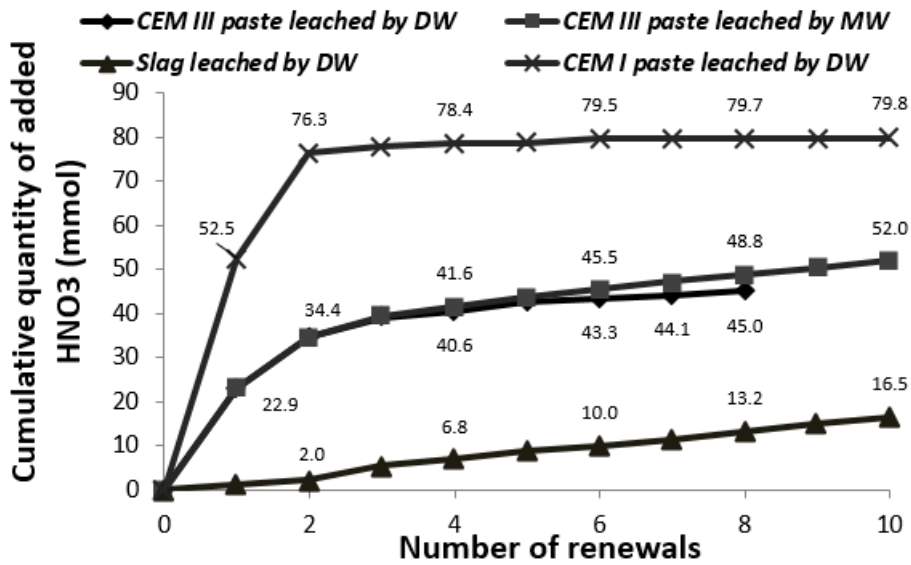
257 *Figure 4: Cumulative concentrations of the leaching elements obtained during the leaching of the slag*
 258 *and of the crushed CEM I paste degraded with demineralised water for one month at 30 °C according*
 259 *to the number of renewals. The values associated with each point correspond to the non-cumulative*
 260 *concentrations (mmol/L) analysed for each leachate.*

261

262 Figure 5 shows the cumulative amount of added nitric acid at each renewal. As in previous results,
 263 the curves obtained for the cementitious pastes have similar patterns, with 95% of the amount of
 264 added HNO₃ being reached at the 2nd renewal for the test conducted on the CEM I paste. From the
 265 3rd renewal, the amount of HNO₃ added in the rest of the test is very small. For the CEM III paste, the
 266 two curves are almost identical until the 4th renewal. At this point, for DW leaching, the amount of
 267 HNO₃ added is very small. For the MW test, the amount of HNO₃ added increases linearly until the
 268 end of the test. For slag leaching, the amount of HNO₃ added is almost linear throughout the test.

269 The monitoring of the addition of HNO₃ between the 1st, 3rd, 5th and last renewals is available in the
 270 supplementary material (Fig. sm1) for the 4 tests conducted.

271



272

273 *Figure 5: Cumulative amount of nitric acid added in the one-month leaching tests according to the*
 274 *number of renewals. The values indicated are the cumulated amounts of nitric acid added.*

275 **3.2. Analysis of degraded materials**

276 Figure 6 shows a SEM backscattered electron mode image of the materials after leaching and Table 4
 277 shows the relative chemical compositions obtained by EDS pointing. The SEM images show a strongly
 278 degraded CEM III paste still containing unreacted slag grains (Figures 6b and 6c). Any clinker grains
 279 observed before leaching (Figure 6a) do not appear to be present after leaching.

280 The EDS analysis of CEM III paste leached with the DW or MW shows a significant degradation
 281 compared to non-leached materials, with a consequent decrease of Ca and S in the cement paste:
 282 the chemical composition decreases from 55.44% to 8.69% for CaO and from 6.37% to 0.50% for SO₃.
 283 This decrease leads to a relative increase in the percentages of SiO₂, Al₂O₃ and MgO due to the 100%
 284 normalization of the quantity of chemical elements analysed. Chemical analysis of the residual slag
 285 present in the CEM III paste also shows a slight loss of calcium and a loss of sulfur. However, the
 286 chemical composition remains very close to that of the unleached slag.

287 XRD mineralogical analyses of the CEM III paste (Figure 7a) show the complete dissolution of the
 288 portlandite, ettringite, C₂S and C₃S initially identified in the unleached paste. Some brownmillerite
 289 (C₄AF) in the clinker is still detected after leaching with DW and MW. In the case of DW leaching,
 290 quartz, originally present in the slag, and hydrotalcite are also identified. A low intensity peak is
 291 observed at 18° but is not identified among the mineral phases of the CEM III cementitious paste. It
 292 was attributed to Teflon (PTFE - Polytetrafluoroethylene), as the Teflon magnet bar used for stirring
 293 was severely degraded due to its abrasion during the test. There was therefore a potential pollution

294 of the cementitious paste by Teflon, as can be seen from the EDS points in areas composed of 98%
295 fluorine. This polymer has a semi-crystalline structure that allows it to be identified by XRD [39], [40].

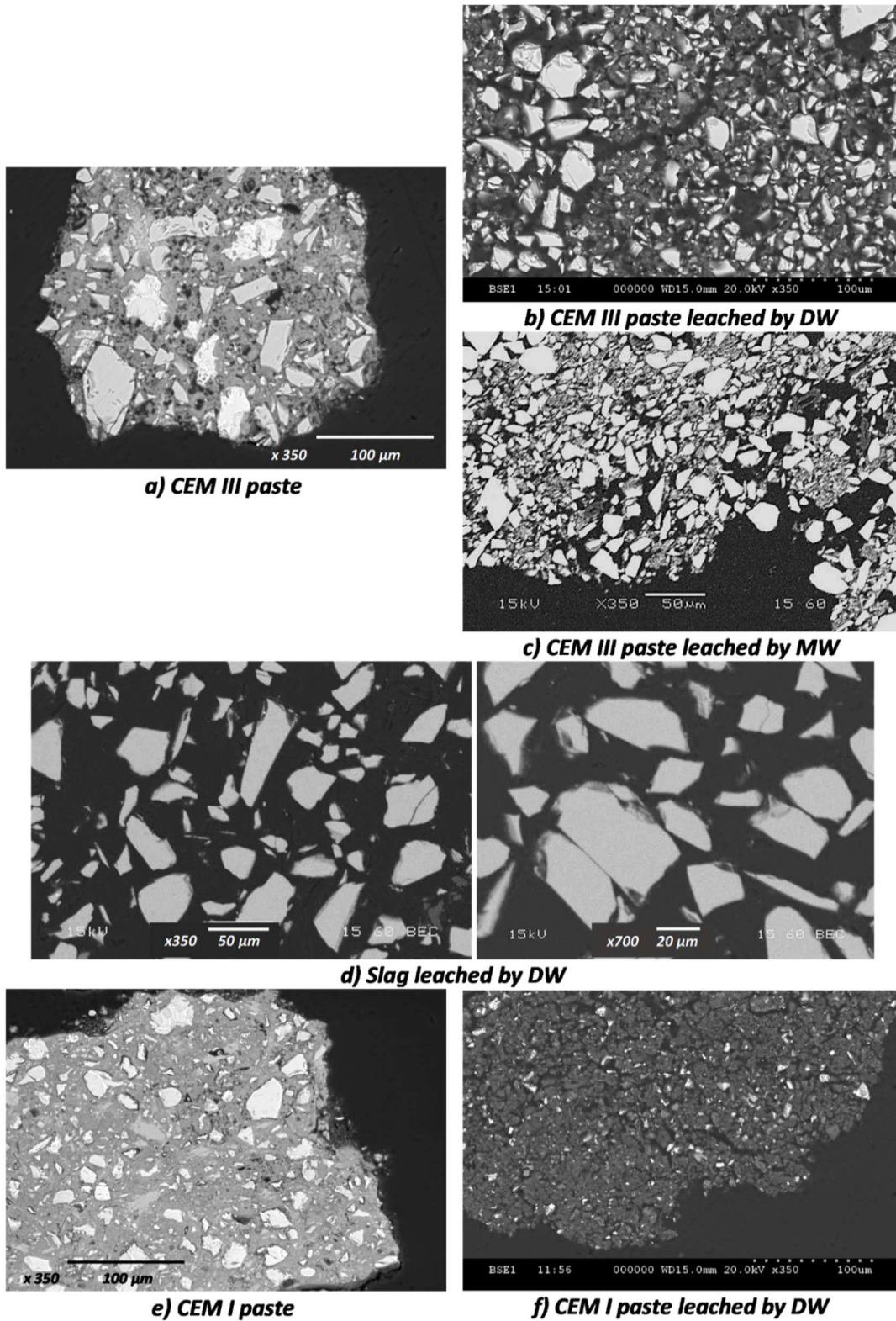
296 The ^{27}Al NMR analysis, in Figure 8, of the CEM III paste before leaching shows the presence of Al in
297 tetrahedral coordination (100/50 ppm range) noted Al^{IV} and Al in octahedral coordination (20/-10
298 ppm range) noted Al^{VI} . The wide signal centred around 60 ppm indicates the presence of Al^{IV} in an
299 amorphous compound. It is characteristic of C-A-S-H and slag. Peaks at 10 and 13 ppm are attributed
300 to AFm and ettringite, respectively [41]. The 5 ppm peak could be attributed to TAH (Third Aluminate
301 Hydrate), a calcium aluminate hydrate or amorphous aluminium hydroxide linked to the formation of
302 C-A-S-H, according to studies conducted by Andersen et al. [42], [43]. The analysis of the CEM III
303 paste after leaching shows a dissolution of the ettringite during leaching in the DW or MW and a
304 change in the shape of the Al^{IV} peak. A peak around 6 ppm is observed for the DW test, which would
305 indicate an increase in the amount of TAH in relation with the increase in the amount of C-A-S-H
306 demonstrated by the displacement of the maximum of the Al^{IV} peak from 65 to 60 ppm. The XRD
307 results obtained also suggest that the peak analysed at 6 ppm could be related to the hydrotalcite
308 observed in XRD, which was poorly crystallized and could have led to a broader NMR peak.

309

310

311 *Table 4: Chemical compositions of crushed CEM III pulp leached with demineralised water and*
 312 *mineralised water, crushed CEM I pulp and slag grains leached with demineralised water for one*
 313 *month. The compositions were obtained by EDS pointing.*

		CaO	SiO ₂	Al ₂ O ₃	SO ₃	MgO	Fe ₂ O ₃
CEM III paste leached by demineralised water	Composition of the leached crushed paste (%mass)	8.69 ± 3.70	53.37 ± 3.59	27.89 ± 2.47	0.50 ± 0.19	7.38 ±3.14	/
	Composition of the degraded slag (%mass)	39.93 ± 1.09	38.31 ± 0.79	12.06 ± 0.56	1.63 ± 0.74	7.32 ± 0.50	/
CEM III paste leached by mineralised water	Composition of the leached crushed paste (%mass)	8.42 ± 3.25	64.72 ± 3.61	19.25 ± 1.02	0.35 ± 0.22	4.76 ± 1.23	/
	Composition of the degraded slag (%mass)	39.06 ± 1.05	38.21 ± 1.30	12.40 ±1.00	1.85 ± 0.27	7.23 ± 0.37	/
Slag leached by demineralised water	Composition of the degraded slag (%mass)	38.62 ± 4.15	40.26 ± 3.82	11.64 ± 1.21	1.84 ± 0.29	6.44 ± 0.94	/
CEM I paste leached by demineralised water	Composition of the leached crushed paste (%mass)	9.70 ± 3.65	53.30 ± 7.96	22.36 ± 3.60	0.28 ± 0.17	1.29 ± 0.51	13.06 ± 4.66
Control materials	Composition of the anhydrous slag (%mass)	43.63 ± 0.76	35.00 ± 0.79	11.58 ± 0.77	2.21 ± 0.68	6.43 ± 0.55	/
	Composition of CEM III paste (%mass)	55.44 ± 2.82	28.91 ± 4.05	4.83 ± 1.53	6.37 ± 2.50	1.29 ± 0.76	/
	Composition of CEM I (%mass)	63.67 ± 5.70	22.99 ± 4.04	4.29 ± 1.82	0.52 ± 0.19	7.06 ± 1.72	1.44 ± 0.69



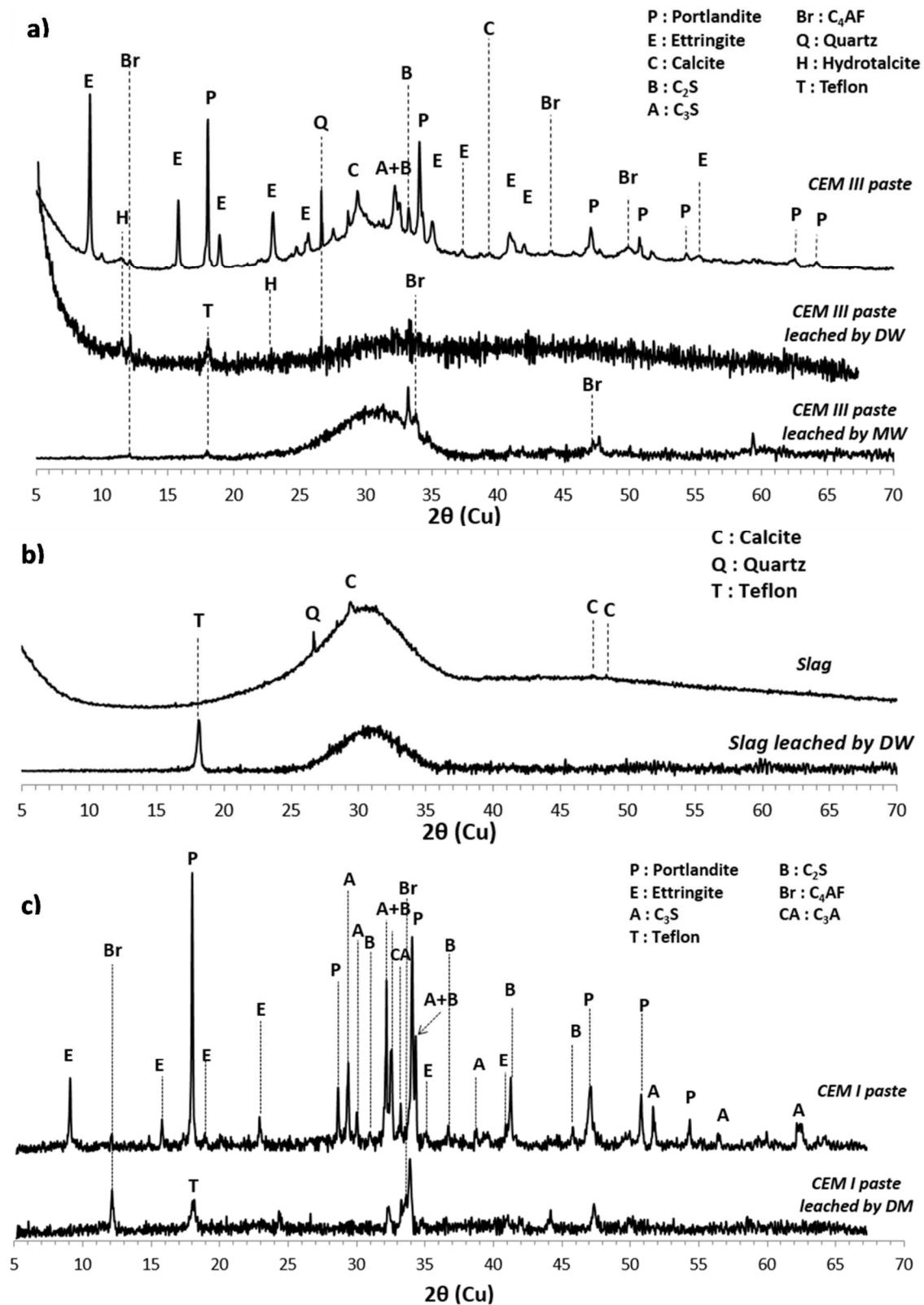
314

315 *Figure 6: Backscattered electron mode SEM image of sound crushed CEM III paste (a), crushed CEM III*
 316 *paste after leaching with demineralised water (b), and after leaching with mineralised water (c);*

317 *crushed slag leached with demineralised water (d); sound crushed CEM I paste (e), after leaching with*
 318 *demineralised water (f).*

319 The SEM images of the leached anhydrous slag (Figure 6d) do not allow any alteration of the slag to
320 be identified via density variations, as the grey level of the grain is homogeneous. As a reminder, the
321 grey level in a back-scattered electron microscopy image reflects density (here, the lighter the grey
322 level, the higher the density of the material). Nevertheless, chemical analysis of the grains by EDS
323 shows a slight decalcification of the slag. In addition, the analysis of the leach solutions showed a
324 calcium release which, considering the initial amount of slag, corresponds to a loss of about 4% of
325 CaO. These results indicate that the variation in the chemical composition of the leached slag
326 analysed by EDS was indeed due to the leaching of the sample and not to the measurement error
327 related to the analytical technique used.

328 The mineralogical analyses performed by XRD on the crushed anhydrous slag before and after
329 demineralised water leaching are shown in Figure 7b. The mineralogical analysis shows essentially
330 the presence of an amorphous phase and a crystallized phase previously identified as Teflon and
331 already observed during the leaching of CEM III cementitious pastes [39], [40]. NMR analysis of ^{27}Al
332 slag before and after leaching seems to show the formation of C-A-S-H (weak displacement of the Al^{IV}
333 peak) but no hydrotalcite (no noticeable peak at the Al^{VI} level).



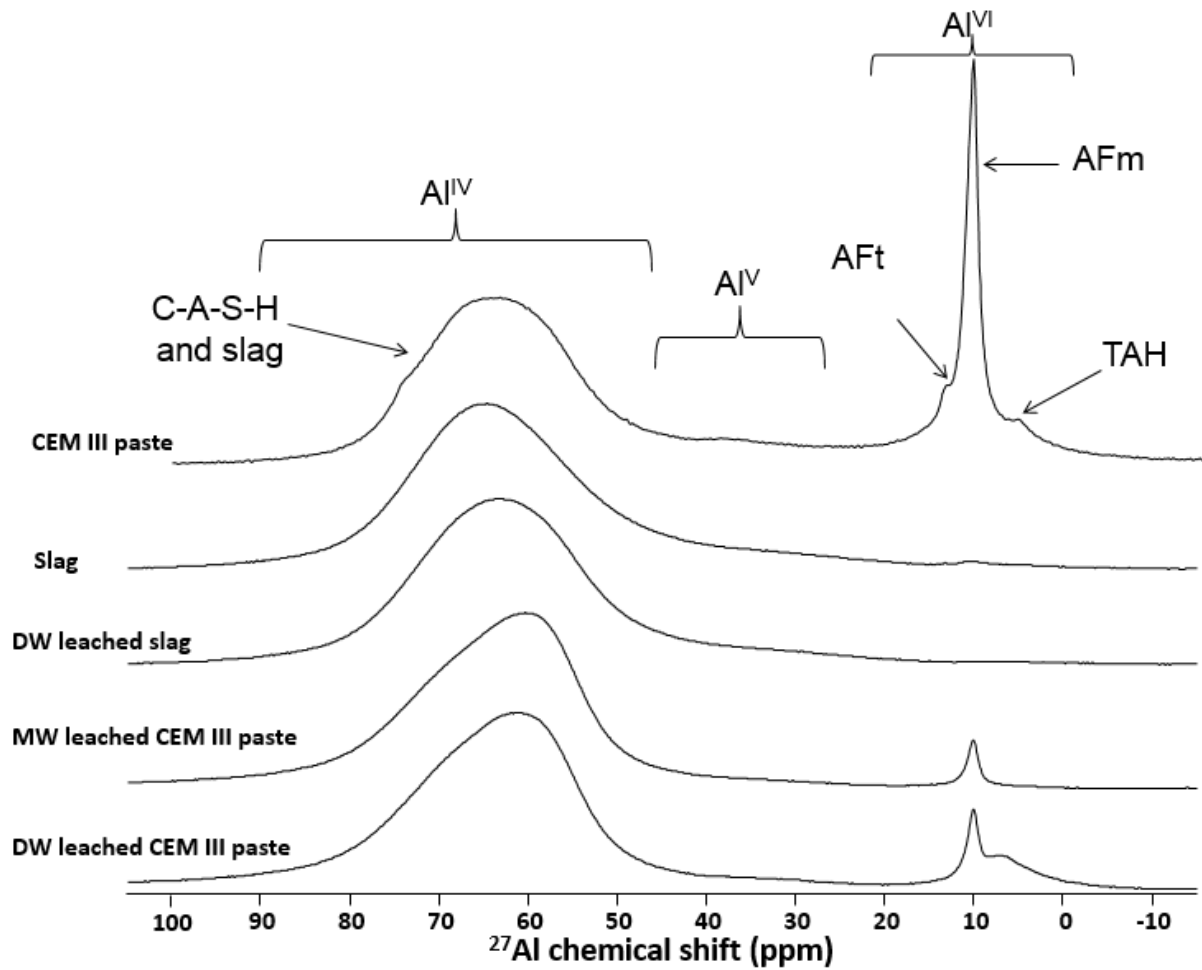
334

335 *Figure 1 : Mineralogical analyses of crushed CEM III paste leached by demineralised and mineralised*
 336 *water (a), crushed slag leached by demineralised water (b), and crushed CEM I paste leached by*
 337 *demineralised water for one month at 30 °C (c) compared to the control samples.*

338 The SEM images presented in Figures 6e and 6f show a backscattered electron mode SEM
339 observation of the crushed CEM I cementitious paste before and after one month of leaching with
340 demineralised water at 30 °C. Unlike the CEM III paste samples, the leached CEM I paste still contains
341 visible clinker grains.

342 EDS chemical analyses performed on the CEM I paste leached by DW showed similar results to those
343 obtained for the CEM III paste leached by DW and MW (Table 4). These results show a strong
344 leaching of calcium and sulfur. Due to the relative nature of chemical analysis, the low percentage of
345 calcium is accompanied by an increase in the percentage of silicon, iron and aluminium. Thus, the
346 composition changes from 63.67% CaO and 7.06% SiO₂ in the unleached CEM I paste to 9.70% CaO
347 and 0.28% SO₃ after leaching.

348 The mineralogical analyses performed on the CEM I paste before and after leaching are shown in
349 Figure 7. They complete the chemical analysis carried out previously and show significant
350 degradation of the material, with the dissolution of ettringite and portlandite and the presence of
351 residual clinker phases after leaching of the material (C₂S, C₃S, C₄AF and C₃A). As in the previous tests,
352 Teflon from the degraded bar magnet was observed [39], [40].



353

354

355

356

Figure 2 : NMR results obtained for crushed CEM III paste leached by demineralised water and demineralised water, and for slag leached by demineralised water. Controls for CEM III paste and slag are also presented.

357

358 4. Discussion

359

360

361

362

It is always difficult to compare leaching tests carried out at constant pH because the amounts of acid added are usually not the same, due to different chemical compositions of the leaching material or solution. However, it is possible to compare the degree of leaching of the different samples by using a Leaching Coefficient (LC) (Equation 1) [44].

$$\begin{aligned}
 LC(t) = & \sum_{i=Ca,Al,Si,Mg} \left[\frac{\text{amount of element } i \text{ leached (mmole) at time } t}{\text{initial amount of element } i \text{ in cement paste (mmole)}} \right. \\
 & \left. \times \frac{\text{molar \% of element } i}{\sum \text{molar \% of Ca, Al, Si, Mg}} \times 100 \right] \quad \text{Eq. 1}
 \end{aligned}$$

363

364 The coefficient is equal to 0 when the cementitious paste is not leached and is equal to 100 when the
365 cementitious paste is completely leached. In the work presented here, the leaching coefficients of
366 calcium, aluminium, silicon and magnesium were taken into account when calculating the leaching
367 coefficient. For leaching tests conducted with mineralised water, the concentrations corrected from
368 initial concentrations in mineral water are used to calculate the leaching coefficient. For tests
369 conducted on crushed samples, the term "*initial amount of element i in the cement paste*" takes a
370 linear loss of mass of the sample throughout the renewals into account according to the following
371 approximation: considering the final mass of the sample after leaching, the loss of mass of the total
372 sample is known and is divided by the number of renewals. Thus, a constant and linear loss of mass
373 at each renewal is assumed.

374 Table 5 presents leaching coefficients obtained at the end of the leaching test for the different
375 elements studied (Ca, Al, Si and Mg). Calcium was found to be the most leached element in all the
376 tests performed. Therefore, for the demineralised water leaching of CEM III, 32.4% of the calcium in
377 the sample was leached, as were 9.2% of the silicon, 2.2% of the magnesium and 1.4% of the
378 aluminium. The percentages obtained for the test carried out with mineralised water follow the same
379 trend but are slightly lower than those obtained with demineralised water. They are 29.1% for
380 calcium, 8.6% for silicon, 1.1% for aluminium and 1.5% for magnesium. The global leaching
381 coefficient is 45% for demineralised water leaching and 40% for mineralised water leaching. On the
382 one hand, this indicates that the CEM III cementitious pastes were strongly degraded under both
383 conditions. On the other hand, the slightly lower leaching coefficients found with mineralised water
384 are probably related to the influence of ions in solution from the mineralised water that modify the
385 chemical conditions in the solution. This difference was also observed by Kamali et al. [11], Hartwich
386 and Vollpracht [20], and Guillon [22] on monolithic cement pastes, in terms of both altered depth
387 and concentrations of released elements. The difference between DW and MW attacks could also be
388 due to the precipitation of secondary phases as a result of chemical reactions between chemical
389 elements of the leachate and those contained in the mineralised water.

390 The slag has a lower percentage of calcium leached by demineralised water (14.9 %) than that
391 obtained for CEM III cementitious paste (32.4 %). The amounts of silicon (8.1 %) and aluminium (0.9
392 %) leached are also slightly lower than for CEM III cementitious paste (9.2 % and 1.4 %, respectively).
393 However, the orders of magnitude are the same for these two chemical elements. The percentage of
394 leached magnesium, in contrast, is higher (2.8% vs. 2.2 %). Overall, the leaching coefficient of the slag

395 leached by demineralised water (26.7%) is lower than that obtained for CEM III cementitious paste
 396 under the same conditions (45%).

397 For CEM I cementitious paste leached with demineralised water, magnesium is the least leached
 398 element (0.6 %). This contrasts with the situation for CEM III paste and slag. 11.8% of silicon and 1%
 399 of aluminium are leached from CEM I in this test. The alteration of the CEM I cementitious paste is
 400 the strongest as shown by its leaching coefficient of 62.6%, which is consistent with a better
 401 durability of the CEM III cementitious matrices than CEM I cementitious matrices [11]–[15], [27].

402 *Table 5: Leaching coefficients obtained for each element (Ca, Al, Mg and Si) at the end of the test for*
 403 *CEM III paste leached by demineralised water and mineralised water, and for slag and CEM I paste*
 404 *leached by demineralised water*

Leaching coefficient	Ca	Si	Al	Mg	Total
CEM III paste leached by DW	32.4	9.2	1.4	2.2	45.2
CEM III paste leached by MW	29.1	8.6	1.1	1.5	40.3
Slag leached by DW	14.9	8.1	0.9	2.8	26.7
CEM I paste leached by DW	49.2	11.8	1.0	0.6	62.6
CEM III paste leached by DW estimated by eq. 1 with $\gamma=31$	25.6	9.3	0.9	2.1	37.9

405
 406 Schiopu studied the leaching of crushed concrete slabs and the influence of pH on the release of
 407 elements [32]. These tests were carried out according to the draft standard on the characterisation
 408 of construction waste, CEN/TS 14429 [33]. Samples of concrete slabs made of CEM I and silico-
 409 calcareous aggregates were crushed to 1 mm and brought into contact with an aqueous acid or basic
 410 solution for 48 hours. The percentage of elements released during the test was determined by
 411 considering the amount released in relation to the initial total content according to the pH. This
 412 quantity can be compared to the calculated leaching coefficients. For a pH of 7.1, the author reports
 413 aluminium, calcium, and silicon leaching rates of 0.07%, 31%, and 3.3%, respectively (magnesium was
 414 not studied). The fact that the percentages are lower than those obtained in this study may be
 415 explained by the shorter test time and coarser particle size of the leached material. However, both
 416 studies show high leaching of calcium followed by that of silicon and, finally, low leaching of
 417 aluminium.

418 Bertron et al. also studied the leaching of crushed CEM I and CEM III cementitious pastes (particle
419 size greater than 2.36 mm) leached with acetic acid solution at an initial pH of 4 [29]. The
420 mechanisms of alteration of the cementitious paste by acetic acid were similar to those observed
421 with a strong acid such as HNO₃ [29]. A leaching percentage was calculated after 6 hours of testing.
422 For CEM I paste, the results showed 14.2% for calcium, 1.1% for silicon, 0.19% for aluminium and
423 3.6% for magnesium. For CEM III cementitious paste, they were respectively 13.3%, 1.65%, 0.94%
424 and 11.8%. Calcium remained the most leached element in the test and aluminium the one with the
425 lowest leaching percentage. Magnesium, however, was strongly leached at pH 4, in contrast to the
426 results obtained in the present study at pH 7.

427 The two leaching tests, conducted by Schiopu and Bertron et al. [29, 32], showed low percentages of
428 leached aluminium. For a CEM III paste, the leaching percentage obtained by Bertron et al. was of
429 0.94 % after 6 hours of testing at pH 4, whereas, in the work reported here, the leaching coefficient
430 obtained for aluminium at pH 7 was 0.008 % after 24 hours of testing, despite a less favourable
431 particle size distribution in the case of Bertron et al.'s tests. This gap can be explained by the
432 difference between the pH values of the tests performed, as found in Lors et al. [44]. Numerous
433 studies, carried out in accordance with CEN/TS 14429, have investigated the variation in the
434 concentration of different leached elements at different pH values (between 3 and 12) [30]–[33],
435 [46]. These tests have shown that concentrations of leached aluminium are high in acidic media, pass
436 through a minimum in neutral media and then increase again in basic media. This phenomenon could
437 thus explain the differences in the percentage leaching obtained for aluminium, which are related to
438 its stability range. This element is in ionic (soluble) form for pH < 6 (Al³⁺ for pH < 4, Al(OH)²⁺ and
439 Al(OH)₂⁺ for pH between 4 and 6), in solid form Al(OH)₃ for pH between 5 and 8, and in ionic form for
440 pH > 8, (Al(OH)₄⁻ for pH between 8 and 11, and Al(OH)₅²⁻ for pH > 11) [46]. This discrepancy may also
441 have been due to the leaching solution used: complexation phenomena between acetate and
442 aluminium could occur and increase aluminium leaching [35], [47], [48]. Magnesium leaching
443 according to pH was also studied by van der Sloot et al. [49], who showed a slightly higher leaching of
444 magnesium at acidic pH than at pH 7, which may explain the difference between Bertron's results
445 [29] and those obtained in the present study for magnesium.

446 The leaching observed for CEM III paste comes from the contribution of cement paste from clinker
447 and slag with a thin layer of hydrates on its surface. These two contributions, which are different, are
448 important for understanding the different stages of the leaching of chemical elements over time.
449 Since the tests carried out do not allow us to trace the origin of the leaching of chemical elements,
450 hypotheses have been used in the aim of determining general trends in the role of cement paste and
451 hydrated slag on the surface. These hypotheses are also based on the use of finely crushed samples,

452 thus reducing the limited influence of diffusion on the leaching kinetics. Thus, as a first
453 approximation, it is considered that the leaching coefficient of the chemical elements of the crushed
454 CEM III paste corresponds to a linear combination of the leaching coefficient of the chemical
455 elements of the crushed CEM I paste and the leaching coefficient of the chemical elements of the
456 crushed slag:

$$457 \quad LC_{\text{CEM III}} = y \times LC_{\text{CEM I}} + (100 - y) \times LC_{\text{Slag}} \quad \text{Eq. 2}$$

458 with y the percentage of clinker in CEM III and LC the total leaching coefficient or that of a chemical
459 element.

460 As the slag in the CEM III paste hydrates on a thin surface layer, the amount of chemical elements
461 released should not exceed that of the slag alone. A CEM III/B contains between 20 and 34 % of
462 clinker, between 80 and 65 % of slag, and between 0 and 5 % of secondary constituents (calcium
463 sulfate). Thus, when CEM III is leached by demineralised water, Equation 2 indicates that the leaching
464 coefficient of a chemical element for CEM III should be between that of slag and that of CEM I,
465 corresponding to $y = 0$ and $y = 100$, respectively. The CEM III leaching coefficients for Ca, Si and Mg
466 are well within the range of leaching coefficients of these elements for CEM I and slag but, for Al, the
467 leaching coefficient is higher than that of slag and also higher than that of CEM I, thus reflecting a
468 more intense Al release mechanism.

469 The MgO content is a good tracer for estimating the respective quantities of clinker (estimated by
470 CEM I) and slag from the CEM III used. Thus, considering the leaching coefficient of Mg (LC Mg Table
471 5), the value of y (clinker content estimated by CEM I) obtained with equation 2 is 27 %. The same
472 value calculated from the leaching coefficient of Si is 30 %. These values of y are well within the
473 range of 20 to 34 %. Furthermore, the composition of CEM III estimated with the chemical
474 compositions of Table 1 gives a value of y equal to 31 % CEM I and 69 % slag, which is a possible
475 composition for a CEM III/B. There is thus an acceptable consistency of these results in view of the
476 approximations made.

477 If we consider the value $y = 31$ % in equation 2, the values of LC Ca, LC Si, LC Al and LC Mg are 25.5,
478 9.3, 0.9 and 2.1 % respectively (Table 5). Thus, Ca is released much more than expected
479 (experimental LC Ca was 32.4 %), Al is released to a lesser extent, and Si and Mg show the expected
480 behaviour (Table 5). The higher Ca release could be due to a higher contribution from the cement
481 paste, indicating higher leaching in the case of CEM III compared to CEM I. This may be the
482 consequence of the smaller amount of clinker and therefore of hydrated cement paste in the CEM III
483 sample, which is nevertheless subject to leaching of similar intensity. This hypothesis is also
484 compatible with an acceleration of Al release. A different reactivity of the residual slag anhydride due

485 to the co-grinding could be another explanation. The slag in CEM III cement is probably finer than the
486 leaching anhydrous slag, and is thus more reactive, i.e. it is more hydrated (more paste available than
487 in the theoretical 70-30 superposition). There are therefore more hydrated phases potentially
488 available for leaching. In addition, if the residual anhydrous slag were to react a little (as the leaching
489 results suggest), their reactivity would be stronger, due to the fineness of the grains.

490 In the case of CEM I and CEM III cement pastes, the leaching coefficient increases very strongly
491 during the first two leachings, then increases much more slowly and almost identically for all other
492 renewals (Figure 9). Thus, it is only after the majority of the calcium contained in the most soluble
493 phases has been leached that the leaching of the other chemical elements becomes significant
494 (Figure 10, Ca leaching coefficient of about 25 % for the leaching of CEM III paste at the second
495 renewal when added to the value of the first renewal). It is therefore imperative to reach a high
496 leaching coefficient to highlight the release of Al. In leaching tests on CEM I cementitious paste,
497 aluminium leaching is not immediate despite the large specific surface area of the crushed sample. A
498 latency time is observed before a higher aluminium leaching rate. At the beginning of the test, Al is
499 leached very little into solution because the Al-containing phases are less soluble than the other
500 phases present, particularly the portlandite. The contribution of these phases to Al leaching becomes
501 visible when their amount in the sample reaches a sufficiently high level, once the more soluble
502 phases have been partially or even completely dissolved. This corresponds to LC values of 50 and 30
503 for CEM I and CEM III respectively. The higher LC value for CEM I has to be related to the higher
504 amount of Ca in this cement compared to CEM III (Table 1) since part of the Ca is associated with the
505 most soluble phases. The Al enrichment of the solid during leaching is well demonstrated by the
506 evolution of the chemical composition of the solid measured by EDS. In the case of the CEM III
507 cementitious paste, this behaviour persists but the latency time is less marked, certainly because of
508 the contribution to leaching of the hydrated slag on its surface, which is present from the beginning
509 of leaching. No latency time is observed for the leaching of Al during the leaching of anhydrous slag
510 (Figure 4).

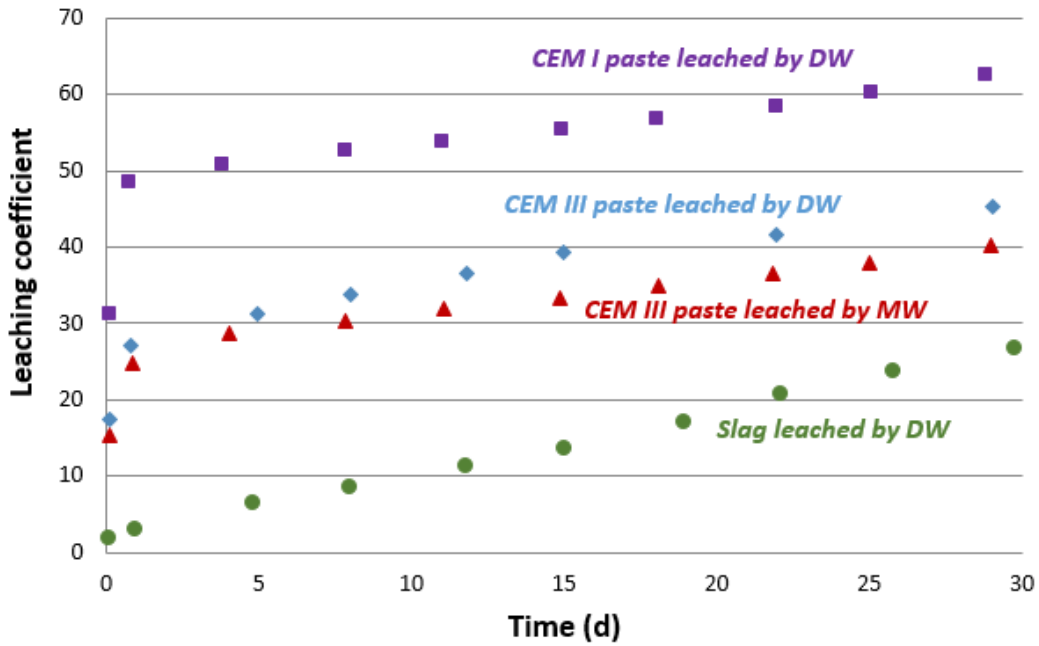
511 The use of a crushed sample in a smaller quantity than the monolithic sample allows a high leaching
512 coefficient to be obtained quickly and thus reduces the latency time before the leaching of Al is
513 observed. The use of a leaching solution having an acidic pH is another way of reducing the latency
514 time for monolithic samples because, apart from AH_3 , the solubility of Al-containing phases increases
515 at lower and lower pH values. Thus, an LC Al of 1.46 is obtained for a CEM I cement-based mortar
516 monolith leached at a constant pH of 2 [45]. This LC Al value is comparable to that obtained for the
517 CEM III but lower: 26.46 instead of the 45.2 obtained in this study. This highlights the increase in the
518 amount of Al leached (as well as the other elements) compared to the amount of Ca leached when

519 the environment is more acidic. The origin of this behaviour is certainly associated with the solubility
520 increase of the Al-containing phases when the pH of the leaching solution decreases. Thus, the LC
521 value necessary to obtain a sizeable release of Al decreases with decreasing pH.

522 These results show that leaching tests leading to low LC only partially describe the mechanism of Al
523 leaching from a cement paste and underestimate leaching. In the case of a CEM I cement paste
524 leached at a constant pH of 7, very little Al is leached in a first step until an LC of 50 for CEM I is
525 reached. This value is 30 for a CEM III paste. This first step can be very long since leaching 50% of a
526 monolithic sample can take a very long time. Nevertheless, once this LC value is exceeded, the
527 release of Al will become much more noteworthy during a second step, which lasts until the phases
528 containing Al have disappeared. In the case of a CEM III paste leached under the same conditions, the
529 contribution of the partially hydrated slag on its surface will be added to the contribution of the
530 cement paste, which can be assimilated to a CEM I paste as a first approximation. Moreover, the
531 presence of slag leads to a lower quantity of Ca in the CEM III. Thus, the Al leaching mechanism for a
532 CEM III paste at pH 7 can be considered to take place in 3 stages. Slag would be the largest
533 contributor to Al leaching for the first and third stages, where LC is less than 30 or very high -
534 corresponding to the total leaching of Al from the cement paste, which then contains only Si,
535 certainly in the form of silica gel with slag certainly still present. In the second step, the main
536 contributor would be the cement paste.

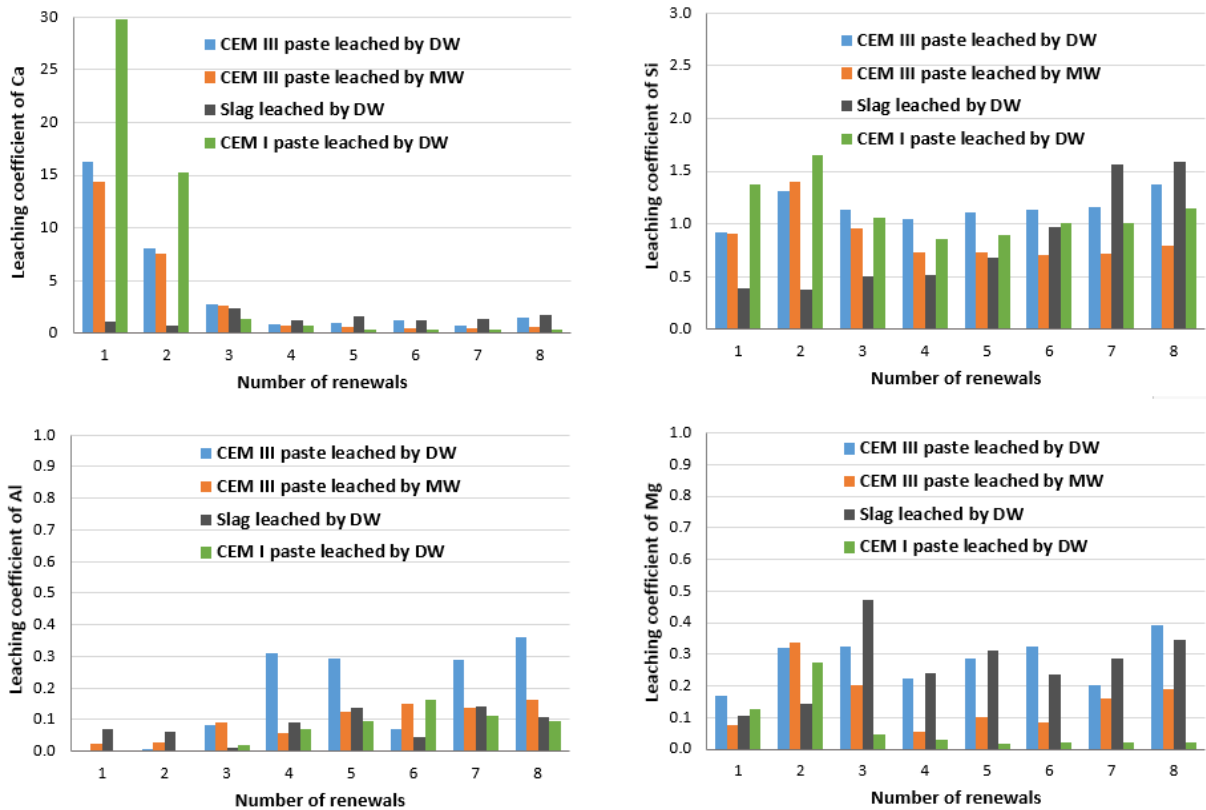
537 However, this Al leaching mechanism must be viewed in the context of a cementitious material used
538 in a drinking water supply pipe. On the one hand, obtaining an LC greater than 30 certainly requires
539 very long exposure times, especially considering the low diffusion coefficient of a CEM III paste and
540 the presence of mineralised water. Practice shows that, in most cases, the very dense microstructure
541 of the CEM III-based cementitious material covering the inside of a cast iron pipe [50] will strongly
542 reduce the leaching kinetics by slowing down diffusion and promoting the formation of a dense layer
543 of mineral phases blocking the porosity [51], especially in the presence of mineralised water. On the
544 other hand, if LC values above 30 were reached, these would certainly be associated with a loss of
545 physical integrity of the cementitious material, leading to a loss of material transported by the water
546 flow, which may lead to other release mechanisms.

547



548

549 *Figure 3 : Leaching coefficients for tests carried out on crushed CEM III cementitious paste leached by*
 550 *demineralised water and mineralised water according to time*



551

552 *Figure 10: Leaching coefficients for Ca, Si, Al and Mg for each leachate renewal, obtained during tests*
 553 *of CEM III cementitious paste leaching with demineralised water and mineralised water, and also for*
 554 *slag and CEM I cementitious paste leached with demineralised water*

555

556 **5. Conclusion**

557 Tests conducted on crushed CEM III pastes maintained at pH 7, in the low pH range of potable water
558 in accordance with the European directive UE 98/83/CE, led to a very high leaching coefficient
559 approaching 50 %. However, despite this high leaching, the amount of Al leached remained very low,
560 i.e. less than 1.5 % of the initial amount of Al in the material. In these experiments, the hydrated slag
561 on the surface, which was rich in Al, tended to release its Al continuously over time, but with slower
562 kinetics than the crushed cement paste. The cement paste released very little Al before the majority
563 of the Ca contained in the most soluble phases had been leached. Then its leaching made a more
564 significant contribution than that of the slag. When the cement paste was almost completely
565 leached, its contribution again became smaller. The leaching of Al from a crushed CEM III paste
566 maintained at pH 7 thus involves 3 steps: (i) a first stage during which the leaching of Al is very slow
567 (LC Al < 0.1 %) and mainly concerns the slag as long as the LC remains below 30 % (value associated
568 with the experimental protocol), (ii) a second stage of significant leaching where the majority
569 contribution comes from the cement paste until its Al is totally consumed, and (iii) a third and final
570 stage (very high LC) during which the leaching of Al is governed by the residual slag and only Si
571 remains present in the cement paste. Thus, a cementitious material that contains a larger amount of
572 Al will not necessarily lead to higher leaching kinetics even if the total amount of Al likely to be
573 leached is initially greater.

574 Despite the use of a crushed material and a high water/material ratio in the leaching tests, the
575 leaching coefficient of Al remains very low here (around 1.4 %). Obtaining a higher leaching
576 coefficient for Al would require a very high number of solution renewals, which is very difficult to
577 achieve experimentally, either on crushed samples or on monoliths. In addition, the impact of the
578 material microstructure on leaching kinetics is greatly reduced with crushed material. The very dense
579 microstructure of a cementitious material based on CEM III will strongly reduce the leaching kinetics
580 by slowing down diffusion and by promoting the formation of a dense layer of mineral phases
581 blocking the porosity in the presence of mineralised water. It is therefore very difficult to perform
582 leaching tests to obtain a high leaching coefficient for Al. Reactive transport modelling would
583 certainly provide additional information on the leaching mechanism if the effect of the
584 microstructure, which is essential to estimate the time needed to reach a given LC value, were
585 associated with it. **Further stages of the study consisted in exposing slag cement-based monolithic
586 mortars to leaching tests under close-to-real conditions in order to assess the range of aluminum
587 concentration in the leachate in relation to regulatory limits.**

588

589

590

591 **Acknowledgements**

592 The authors wish to thank Saint-Gobain Recherche Paris and Saint-Gobain PAM for their technical
593 and financial support.

594

595 **References**

596 [1] C. Gourier-Fréry et al., « Aluminium. Quels risques pour la santé ? Synthèse des études
597 épidémiologiques. Volet épidémiologique de l'expertise collective InVS-Afssa-Afssaps », Institut de
598 veille sanitaire, Nov. 2003.

599 [2] D. R. Crapper McLachlan, Aluminum and alzheimer's disease », *Neurobiol. Aging*, vol. 7, no 6,
600 p. 525-532, Nov. 1986, doi: 10.1016/0197-4580(86)90102-8.

601 [3] S. Maya, T. Prakash, K. D. Madhu, and D. Goli, Multifaceted effects of aluminium in
602 neurodegenerative diseases: A review, *Biomed. Pharmacother.*, vol. 83, p. 746-754, Oct. 2016, doi:
603 10.1016/j.biopha.2016.07.035.

604 [4] V. Rondeau, D. Commenges, H. Jacqmin-Gadda, and J.-F. Dartigues, Relation between
605 Aluminum Concentrations in Drinking Water and Alzheimer's Disease: An 8-year Follow-up Study,
606 *Am. J. Epidemiol.*, vol. 152, no 1, p. 59-66, Jan. 2000, doi: 10.1093/aje/152.1.59.

607 [5] Z. Wang et al., Chronic exposure to aluminum and risk of Alzheimer's disease: A meta-
608 analysis, *Neurosci. Lett.*, vol. 610, p. 200-206, Jan. 2016, doi: 10.1016/j.neulet.2015.11.014.

609 [6] A. Mirza, A. King, C. Troakes, and C. Exley, Aluminium in brain tissue in familial Alzheimer's
610 disease, *J. Trace Elem. Med. Biol.*, vol. 40, p. 30-36, mars Mar. 2017, doi:
611 10.1016/j.jtemb.2016.12.001.

612 [7] E. Gauthier, I. Fortier, F. Courchesne, P. Pepin, J. Mortimer, and D. Gauvreau, Aluminum
613 Forms in Drinking Water and Risk of Alzheimer's Disease, *Environ. Res.*, vol. 84, no 3, p. 234-246,
614 Nov. 2000, doi: 10.1006/enrs.2000.4101.

615 [8] World Health Organization, Guidelines for drinking-water quality, 4th edition, incorporating
616 the 1st addendum, 2017, ISBN: 978-92-4-254995-9.

- 617 [9] AFNOR, NF EN 197-1 Ciment - Partie 1 : Composition, spécifications et critères de conformité
618 des ciments courants, 2012.
- 619 [10] G. J. Osborne, Durability of Portland blast-furnace slag cement concrete, *Cem. Concr.*
620 *Compos.*, vol. 21, no 1, p. 11-21, Jan. 1999, doi: 10.1016/S0958-9465(98)00032-8.
- 621 [11] S. Kamali, M. Moranville, and S. Leclercq, Material and environmental parameter effects on
622 the leaching of cement pastes: Experiments and modelling, *Cem. Concr. Res.*, vol. 38, no 4, p.
623 575-585, Apr. 2008.
- 624 [12] E. Rozière and A. Loukili, Performance-based assessment of concrete resistance to leaching,
625 *Cem. Concr. Compos.*, vol. 33, no 4, p. 451-456, Apr. 2011, doi: 10.1016/j.cemconcomp.2011.02.002.
- 626 [13] W. Müllauer, R. E. Beddoe, and D. Heinz, Leaching behaviour of major and trace elements
627 from concrete: Effect of fly ash and GGBS, *Cem. Concr. Compos.*, vol. 58, p. 129-139, Apr. 2015, doi:
628 10.1016/j.cemconcomp.2015.02.002.
- 629 [14] Y.-J. Tang, X.-B. Zuo, S.-L. He, O. Ayinde, and G.-J. Yin, Influence of slag content and water-
630 binder ratio on leaching behavior of cement pastes, *Constr. Build. Mater.*, vol. 129, p. 61-69, Dec.
631 2016, doi: 10.1016/j.conbuildmat.2016.11.003.
- 632 [15] A. Bertron, G. Escadeillas, and J. Duchesne, Cement pastes alteration by liquid manure
633 organic acids: chemical and mineralogical characterization, *Cem. Concr. Res.*, vol. 34, no 10, p.
634 1823-1835, Oct. 2004, doi: 10.1016/j.cemconres.2004.01.002.
- 635 [16] P. Faucon, F. Adenot, M. Jorda, and R. Cabrillac, Behaviour of crystallised phases of Portland
636 cement upon water attack, *Mater. Struct.*, vol. 30, no 8, p. 480-485, Oct. 1997, doi:
637 10.1007/BF02524776.
- 638 [17] K. Haga, S. Sutou, M. Hironaga, S. Tanaka, and S. Nagasaki, Effects of porosity on leaching of
639 Ca from hardened ordinary Portland cement paste, *Cem. Concr. Res.*, vol. 35, no 9, p. 1764-1775,
640 Sept. 2005, doi: 10.1016/j.cemconres.2004.06.034.
- 641 [18] F. Han, R. Liu, and P. Yan, Effect of fresh water leaching on the microstructure of hardened
642 composite binder pastes, *Constr. Build. Mater.*, vol. 68, p. 630-636, Oct. 2014, doi:
643 10.1016/j.conbuildmat.2014.07.019.
- 644 [19] K. Wan, Y. Li, and W. Sun, Experimental and modelling research of the accelerated calcium
645 leaching of cement paste in ammonium nitrate solution, *Constr. Build. Mater.*, vol. 40, p. 832-846,
646 Mar. 2013, doi: 10.1016/j.conbuildmat.2012.11.066.

- 647 [20] A. Vollpracht and W. Brameshuber, Binding and leaching of trace elements in Portland
648 cement pastes, *Cem. Concr. Compos.*, vol. 79, p. 76-92, Jan. 2016.
- 649 [21] P. Hartwich and A. Vollpracht, Influence of leachate composition on the leaching behaviour
650 of concrete, *Cem. Concr. Res.*, vol. 100, p. 423-434, Oct. 2017, doi:
651 10.1016/j.cemconres.2017.07.002.
- 652 [22] E. Guillon, Durabilité des matériaux cimentaires - Modélisation de l'influence des équilibres
653 physico-chimiques sur la microstructure et les propriétés mécaniques résiduelles, 2004.
- 654 [23] P. Faucon, F. Adenot, J. F. Jacquinet, J. C. Petit, R. Cabrillac, and M. Jorda, Long-term
655 behaviour of cement pastes used for nuclear waste disposal: review of physico-chemical mechanisms
656 of water degradation, *Cem. Concr. Res.*, vol. 28, no 6, p. 847-857, Jun. 1998, doi: 10.1016/S0008-
657 8846(98)00053-2.
- 658 [24] F. Adenot and M. Buil, Modelling of the corrosion of the cement paste by deionized water,
659 *Cem. Concr. Res.*, vol. 22, no 2-3, p. 489-496, Mar. 1992, doi: 10.1016/0008-8846(92)90092-A.
- 660 [25] P. Faucon et al., Leaching of cement: Study of the surface layer, *Cem. Concr. Res.*, vol. 26, no
661 11, p. 1707-1715, Nov. 1996, doi: 10.1016/S0008-8846(96)00157-3.
- 662 [26] R. B. Kogbara and A. Al-Tabbaa, Mechanical and leaching behaviour of slag-cement and lime-
663 activated slag stabilised/solidified contaminated soil, *Sci. Total Environ.*, vol. 409, no 11, p.
664 2325-2335, mai May 2011, doi: 10.1016/j.scitotenv.2011.02.037.
- 665 [27] M. O'Connell, C. McNally, and M. G. Richardson, Performance of concrete incorporating
666 GGBS in aggressive wastewater environments, *Constr. Build. Mater.*, vol. 27, no 1, p. 368-374, Feb.
667 2012, doi: 10.1016/j.conbuildmat.2011.07.036.
- 668 [28] J. Duchesne and A. Bertron, Leaching of cementitious materials by pure water and strong
669 acids (HCl and HNO₃), in *Performance of cement-based materials in aggressive aqueous*
670 *environments*, Springer, 2013, p. 91-112.
- 671 [29] A. Bertron, J. Duchesne, and G. Escadeillas, Attack of cement pastes exposed to organic acids
672 in manure, *Cem. Concr. Compos.*, vol. 27, no 9-10, p. 898-909, Oct. 2005, doi:
673 10.1016/j.cemconcomp.2005.06.003.
- 674 [30] C. J. Engelsens, H. A. van der Sloot, G. Wibetoe, G. Petkovic, E. Stoltenberg-Hansson, and W.
675 Lund, Release of major elements from recycled concrete aggregates and geochemical modelling,
676 *Cem. Concr. Res.*, vol. 39, no 5, p. 446-459, May 2009, doi: 10.1016/j.cemconres.2009.02.001.

- 677 [31] M. Lupsea, L. Tiruta-Barna, and N. Schiopu, Leaching of hazardous substances from a
678 composite construction product – An experimental and modelling approach for fibre-cement sheets,
679 *J. Hazard. Mater.*, vol. 264, p. 236-245, Jan. 2014, doi: 10.1016/j.jhazmat.2013.11.017.
- 680 [32] N. Schiopu, *Caractérisation des émissions dans l'eau des produits de construction pendant*
681 *leur vie en oeuvre*, INSA Lyon, 2007.
- 682 [33] Comité Européen de Normalisation (CEN), XP CEN/TS 14429 Characterization of waste -
683 leaching behaviour tests - influence of pH on leaching with initial acid/base addition, 2006.
- 684 [34] F. Adenot, *Durabilité du béton : caractérisation et modélisation des processus physiques et*
685 *chimiques de dégradation du ciment*, Université d'Orléans, 1992.
- 686 [35] A. P. Black and D. G. Willems, *Electrophoretic Studies of Coagulation for Removal of Organic*
687 *Color*, *J. Am. Water Works Assoc.*, vol. 53, no 5, p. 589-604, 1961.
- 688 [36] D. Damidot, S. J. Barnett, F. P. Glasser, et D. E. Macphee, « Investigation of the CaO–Al₂O₃–
689 SiO₂–CaSO₄–CaCO₃–H₂O system at 25°C by thermodynamic calculation », *Adv. Cem. Res.*, vol. 16, no
690 2, p. 69-76, avr. 2004, doi: 10.1680/adcr.2004.16.2.69.
- 691 [37] D. Jacques, L. Wang, E. Martens, et D. Mallants, « Modelling chemical degradation of
692 concrete during leaching with rain and soil water types », *Cem. Concr. Res.*, vol. 40, no 8, p.
693 1306-1313, août 2010, doi: 10.1016/j.cemconres.2010.02.008.
- 694 [38] J. Olmeda, P. Henocq, E. Giffaut, et M. Grivé, « Modelling of chemical degradation of blended
695 cement-based materials by leaching cycles with Callovo-Oxfordian porewater », *Phys. Chem. Earth*
696 *Parts ABC*, vol. 99, p. 110-120, juin 2017, doi: 10.1016/j.pce.2017.05.008.
- 697 [39] X. L. Huang, *Etude de l'évolution de la morphologie et des propriétés électriques du*
698 *polytétrafluoroéthylène (PTFE) pour des applications aéronautiques en hautes températures (250 –*
699 *400 °C)*, Université de Toulouse, 2014.
- 700 [40] A. Atta and H. Ali, *Structural and Thermal Properties of PTFE Films by Argon and Oxygen*
701 *Plasma*, *Arab J. Nucl. Sci. Appl.*, vol. 46, no 5, p. 106-114, 2013.
- 702 [41] R. Taylor, I. G. Richardson, and R. M. D. Brydson, *Composition and microstructure of 20-year-*
703 *old ordinary Portland cement–ground granulated blast-furnace slag blends containing 0 to 100% slag*,
704 *Cem. Concr. Res.*, vol. 40, no 7, p. 971-983, Jul. 2010, doi: 10.1016/j.cemconres.2010.02.012.

- 705 [42] M. D. Andersen, H. J. Jakobsen, and J. Skibsted, Incorporation of Aluminum in the Calcium
706 Silicate Hydrate (C–S–H) of Hydrated Portland Cements: A High-Field ²⁷Al and ²⁹Si MAS NMR
707 Investigation, *Inorg. Chem.*, vol. 42, no 7, p. 2280-2287, Apr. 2003, doi: 10.1021/ic020607b.
- 708 [43] M. D. Andersen, H. J. Jakobsen, and J. Skibsted, A new aluminium-hydrate species in hydrated
709 Portland cements characterized by ²⁷Al and ²⁹Si MAS NMR spectroscopy, *Cem. Concr. Res.*, vol. 36,
710 no 1, p. 3-17, Jan. 2006, doi: 10.1016/j.cemconres.2005.04.010.
- 711 [44] C. Lors, E. D. Hondjuila Miokono, and D. Damidot, Interactions between *Halothiobacillus*
712 *neapolitanus* and mortars: Comparison of the biodeterioration between Portland cement and
713 calcium aluminate cement, *Int. Biodeterior. Biodegrad.*, vol. 121, p. 19-25, Jul. 2017, doi:
714 10.1016/j.ibiod.2017.03.010.
- 715 [45] C. Lors and D. Damidot, Long term leaching experiments of OPC mortars at constant pH in
716 acidic conditions, *Proceedings of the 14th International Congress on the Chemistry of cement, Beijing*
717 *(Chinae)*, 2015.
- 718 [46] A. Keulen, A. van Zomeren, and J. J. Dijkstra, Leaching of monolithic and granular alkali
719 activated slag-fly ash materials, as a function of the mixture design, *Waste Manag.*, vol. 78, p.
720 497-508, août Aug. 2018, doi: 10.1016/j.wasman.2018.06.019.
- 721 [47] L. De Windt and P. Devillers, Modeling the degradation of Portland cement pastes by
722 biogenic organic acids, *Cem. Concr. Res.*, vol. 40, no 8, p. 1165-1174, août Aug. 2010, doi:
723 10.1016/j.cemconres.2010.03.005.
- 724 [48] L. De Windt, A. Bertron, S. Larreur-Cayol, and G. Escadeillas, Interactions between hydrated
725 cement paste and organic acids: Thermodynamic data and speciation modeling, *Cem. Concr. Res.*,
726 vol. 69, p. 25-36, Mar. 2015, doi: 10.1016/j.cemconres.2014.12.001.
- 727 [49] H. A. van der Sloot, Comparison of the characteristic leaching behavior of cements using
728 standard (EN 196-1) cement mortar and an assessment of their long-term environmental behavior in
729 construction products during service life and recycling, *Cem. Concr. Res.*, vol. 30, no 7, p. 1079-1096,
730 Jul. 2000, doi: 10.1016/S0008-8846(00)00287-8.
- 731 [50] M. Berthomier, Etude de la lixiviation de matériaux cimentaires à bas de CEM III utilisés dans
732 les canalisations d'eau potable : approche expérimentale et numérique, PhD thesis, INSA Toulouse,
733 2019.

734 [51] M. Schwotzer, T. Scherer, and A. Gerdes, Protective or damage promoting effect of calcium
735 carbonate layers on the surface of cement based materials in aqueous environments, Cem. Concr.
736 Res., vol. 40, no 9, p. 1410-1418, Sept. 2010, doi: 10.1016/j.cemconres.2010.05.001.

737